



# Exploring the inhibitory activity and mechanism on lipid production in 3T3-L1 cells by hot water extract derived from *Acacia confusa* flowers

Nai-Wen Tsao<sup>1</sup> · Ju-Ya Cheng<sup>2</sup> · Sheng-Yang Wang<sup>1,2,3</sup>

Received: 10 June 2024 / Accepted: 17 October 2024

© The Author(s) under exclusive licence to The Japanese Society of Pharmacognosy 2024

## Abstract

*Acacia confusa* Merr. (Fabaceae) (*A. confusa*) is a native tree species of Taiwan, commonly found in the low-altitude mountains and hilly areas of the Hengchun Peninsula. This evergreen, perennial, and large-sized tree was the focus of a study that employed various chromatographic and spectroscopic methods to analyze the hot water extract of its flowers. The analysis revealed that the major components of the extract were myricitrin, quercitrin, europetin-3-*O*-rhamnoside, and chalconaringenin-2'-xyloside, with respective concentrations of approximately 0.22, 0.02, 0.26, and 0.10 mg/g of the flowers. Subsequent cell assays were conducted to assess the inhibitory effect of the extract on lipid synthesis in fat cells. Oil Red O staining results indicated that the extract significantly suppressed fatty acid accumulation in 3T3-L1 cells, with the most pronounced effect observed at a concentration of 180 µg/ml. Furthermore, the hot water extract of *A. confusa* flowers was found to increase the phosphorylation of AMP-activated protein kinase (AMPK), decrease the phosphorylation of cAMP response element-binding protein (CREB), and reduce the expression of glucocorticoid receptor (GR) protein. This, in turn, inhibited the expression of downstream transcription factors such as CCAT/ehancer binding proteins  $\alpha$  (C/EBP $\alpha$ ), CCAT/ehancer binding proteins  $\beta$  (C/EBP $\beta$ ), CCAT/ehancer binding proteins  $\delta$  (C/EBP $\delta$ ), peroxisome proliferation-activated receptor  $\gamma$  (PPAR $\gamma$ ), and sterol regulatory element binding proteins-1 (SREBP-1). Consequently, the expression of lipid synthesis-related proteins acetyl-CoA carboxylase (ACC), fatty acid synthase (FAS), and fatty acid translocase (CD36) was reduced, ultimately inhibiting lipid generation. Therefore, the hot water extract of *A. confusa* flowers shows potential for development as a weight-loss tea.

---

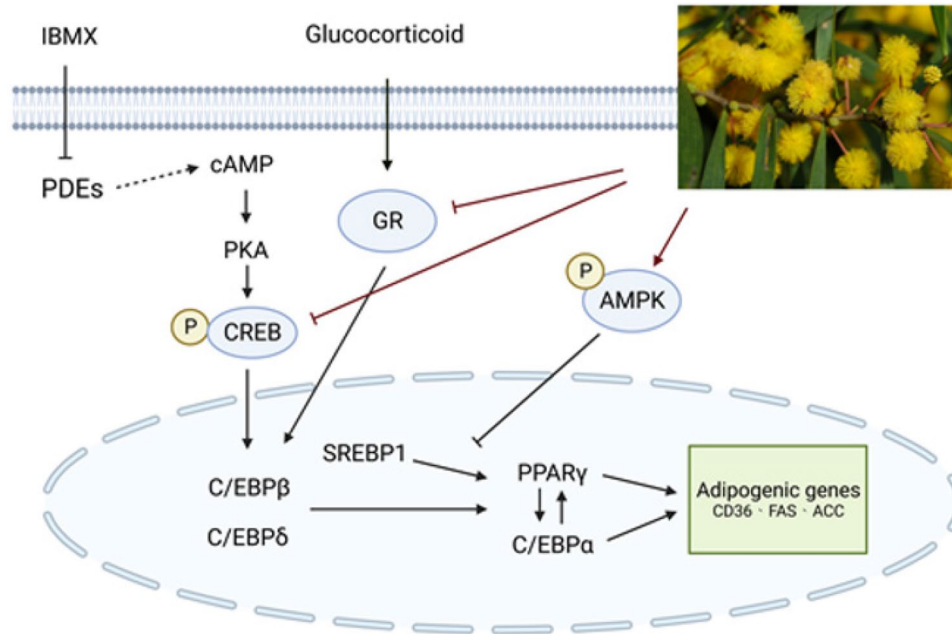
✉ Sheng-Yang Wang  
taiwanfir@dragon.nchu.edu.tw

<sup>1</sup> Department of Forestry, National Chung-Hsing University,  
250 Kuo-Kuang Road, Taichung 402, Taiwan

<sup>2</sup> Program in Special Crop and Metabolome, Academy  
of Circle Economy, National Chung Hsing University,  
Nantou 540, Taiwan

<sup>3</sup> Agricultural Biotechnology Research Center, Academia  
Sinica, Taipei 108, Taiwan

## Graphical abstract



**Keywords** *Acacia confusa* · Flowers · Extractives · Flavonoids · 3T3-L1 cell

## Introduction

Due to shifts in contemporary dietary and lifestyle habits, prolonged sedentary behavior, and the consumption of high-fat, high-calorie foods, the global obese population has rapidly escalated. Estimates from the World Federation of Obesity predict that by 2035, the worldwide obese population will reach 1.9 billion, accounting for one in every four individuals. The economic ramifications of addressing obesity and overweight on a global scale are projected to be as high as 4.32 trillion US dollars. Various methods for treating obesity exist, including pharmaceuticals and surgery. However, dietary therapy and exercise stand out as options with fewer side effects and greater safety. Consequently, this experiment utilizes the flowers of the natural plant *Acacia confusa* (Fabaceae) (*A. confusa*) as the experimental material. *A. confusa* is a native species of Taiwan, widely distributed in low-altitude mountainous and hilly areas. According to the Forest Resource Inventory by the Forestry and Nature Conservation Agency, *A. confusa* covers 14,780 hectares in artificial forests, with an accumulated volume of 1.54 million cubic meters, making it the most abundant species in artificial broad-leaved forests in terms *A. confusa* that can be harnessed for this purpose.

When considering the properties of *A. confusa* wood, its inherent density has traditionally made it a preferred material for fuel and charcoal. Additionally, due to its rapid

growth and resilience in diverse environmental conditions—including dry, humid, and windy settings—it has consistently been chosen as one of the primary tree species for early-stage afforestation. Research has highlighted various biological activities associated with *A. confusa* extracts, including antioxidant and free radical scavenging properties, hepatoprotective effects, xanthine oxidase inhibition, aminoisobutyric acid-sensitive amine oxidase inhibition, angiotensin I-converting enzyme inhibition, anti-hyperuricemic effects, and anti-inflammatory activities [1–8]. Despite extensive investigations into the biological activities of *A. confusa* extracts, there is a notable lack of research on its potential to inhibit lipid accumulation. Therefore, this study specifically focuses on the hot water extract derived from *A. confusa* flowers (ACF). It aims to analyse the composition of the extract and evaluate its effectiveness in inhibiting lipid generation in fat cells through cell culture methods.

## Results and discussion

The yield of ACF hot water extract was approximately 6.02%. Figure 1 shows the UV fingerprint chromatogram obtained by HPLC analysis 360 nm. Four compounds (1–4, Fig. 2) were collected, purified, and subjected to NMR analysis for structural identification.

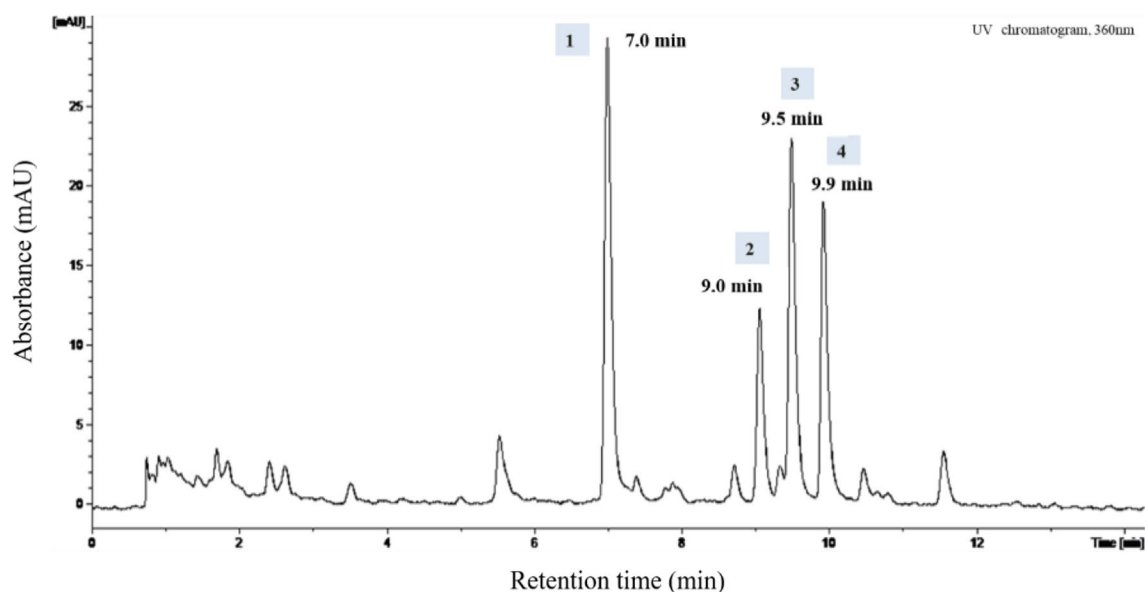


Fig. 1 The HPLC chromatogram of *A. confusa* flowers hot water extract

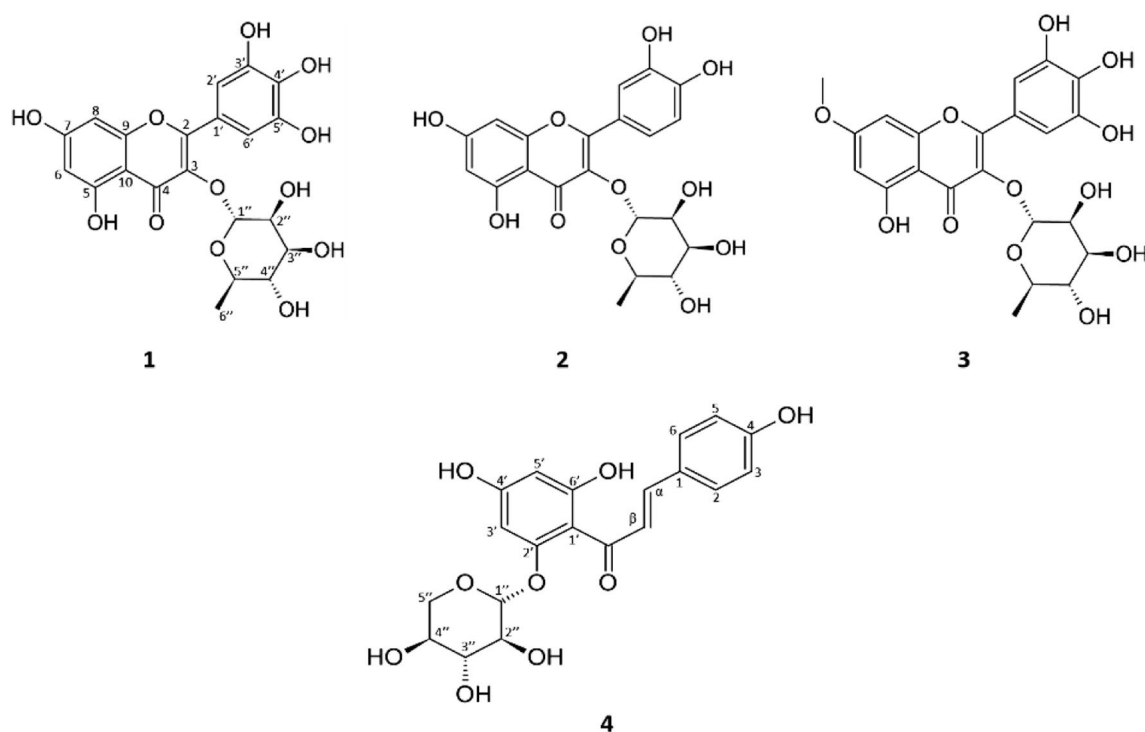


Fig. 2 Structures of myricitrin (1), quercitrin (2), europetin-3-*O*-rhamnoside (3), and chalconaringenin-2'-xyloside (4) from *A. confusa* flowers

Compounds **1** and **2** were identified as myricitrin and quercitrin, respectively [9, 10]. They exhibited similar NMR and MS data (Table 1), consistent with their structural similarity, differing only in the substitution pattern of the B-ring. The key differences were the presence of two meta-oriented aromatic protons in the B-ring of myricitrin [ $\delta_{\text{H}}$  6.95 (2H,

s, H-2' and H-6')], while quercitrin showed an ABX system [ $\delta_{\text{H}}$  7.34 (1H, d,  $J=2.0$  Hz, H-2'), 7.31 (1H, dd,  $J=8.4$ , 2.0 Hz, H-6'), and 6.91 (1H, d,  $J=8.4$  Hz, H-5')]. Compound **3**, identified as europetin-3-*O*-rhamnoside, showed similar NMR and MS data (Table 1) to compounds **1** and **2** [9, 11]. However, it was distinguished by the presence of a

**Table 1**  $^1\text{H}$  and  $^{13}\text{C}$  NMR chemical shift data analysis result of compounds **1–3** ( $\delta$  in ppm,  $J$  in Hz, 400 and 100 MHz in  $\text{CD}_3\text{OD}$ )

| Position       | 1                   |                     | 2                   |                     | 3                   |                     |
|----------------|---------------------|---------------------|---------------------|---------------------|---------------------|---------------------|
|                | $\delta_{\text{C}}$ | $\delta_{\text{H}}$ | $\delta_{\text{C}}$ | $\delta_{\text{H}}$ | $\delta_{\text{C}}$ | $\delta_{\text{H}}$ |
| 2              | 159.6               |                     | 159.5               |                     | 159.9               |                     |
| 3              | 136.5               |                     | 136.4               |                     | 136.6               |                     |
| 4              | 179.8               |                     | 179.8               |                     | 179.9               |                     |
| 5              | 163.4               |                     | 163.4               |                     | 163.1               |                     |
| 6              | 100.0               | 6.20 d (2.0)        | 100.0               | 6.21 d (2.2)        | 99.1                | 6.34 d (2.2)        |
| 7              | 166.1               |                     | 166.1               |                     | 167.4               |                     |
| 8              | 94.8                | 6.37 d (2.0)        | 94.9                | 6.38 d (2.2)        | 93.2                | 6.56 d (2.2)        |
| 9              | 158.7               |                     | 158.7               |                     | 158.5               |                     |
| 10             | 106.0               |                     | 106.0               |                     | 106.9               |                     |
| 1'             | 122.1               |                     | 123.0               |                     | 121.9               |                     |
| 2'             | 109.7               | 6.95 s              | 117.1               | 7.34 d (2.0)        | 109.8               | 6.97 s              |
| 3'             | 147.0               |                     | 146.6               |                     | 147.0               |                     |
| 4'             | 138.0               |                     | 150.0               |                     | 138.2               |                     |
| 5'             | 147.0               |                     | 116.5               | 6.91 d (8.4)        | 147.0               |                     |
| 6'             | 109.7               | 6.95 s              | 123.1               | 7.31 dd (8.4, 2.0)  | 109.8               | 6.97 s              |
| 1''            | 103.8               | 5.31 d (1.5)        | 103.7               | 5.35 d (1.6)        | 103.8               | 5.33 d (1.4)        |
| 2''            | 72.0                | 4.22 dd (3.3, 1.5)  | 72.1                | 4.22 dd (3.2, 1.6)  | 72.0                | 4.22 dd (3.2, 1.4)  |
| 3''            | 72.3                | 3.79 dd (9.5, 3.3)  | 72.3                | 3.75 dd (9.2, 3.2)  | 72.3                | 3.80 dd (9.5, 3.2)  |
| 4''            | 73.5                | 3.34 t (9.5)        | 73.4                | 3.35 t (9.2)        | 73.5                | 3.34 t (9.5)        |
| 5''            | 72.2                | 3.51 m              | 72.2                | 3.42 m              | 72.2                | 3.52 m              |
| 6''            | 17.8                | 0.96 d (6.2)        | 17.8                | 0.94 d (6.4)        | 17.8                | 0.97 d (6.2)        |
| $\text{OCH}_3$ |                     |                     |                     |                     | 56.6                | 3.88 s              |

methoxy group [ $\delta_{\text{H}}$  3.88 (3H, s)] ( $\delta_{\text{H}}$  3.88 (3H, s,  $-\text{OCH}_3$ ), which downfield shift of this methoxy signal suggests that it is attached to an aromatic ring.

Compound **4** exhibited  $[\text{M}-\text{H}]^-$  ion at  $m/z$  403.0 in the ESI-MS spectrum. The loss of mass of  $m/z$  132, resulting in a fragment at  $m/z$  271.3, corresponding to the loss of a pentose unit from the parent ion. This fragmentation pattern is consistent with the presence of a pentose glycoside moiety [12]. The  $^1\text{H}$  NMR spectrum ( $\text{CD}_3\text{OD}$ , 400 MHz, Table 2) showed two *para*-disubstituted aromatic protons [ $\delta_{\text{H}}$  7.59 (2H, d,  $J=8.6$  Hz, H-2 and H-6) and 6.83 (2H, d,  $J=8.6$  Hz, H-3 and H-5)], two *meta*-oriented aromatic protons [ $\delta_{\text{H}}$  6.16 (1H, d,  $J=2.4$  Hz, H-3') and 5.99 (1H, d,  $J=2.4$  Hz, H-5')], the disubstituted double bond protons [ $\delta_{\text{H}}$  7.99 (1H, d,  $J=15.4$  Hz, H- $\alpha$ ) and 7.67 (1H, d,  $J=15.4$  Hz, H- $\beta$ )], suggesting a *trans* double bond configuration, and the glycoside protons [ $\delta_{\text{H}}$  5.08 (1H, d,  $J=7.3$  Hz, H-1''), 3.97 (1H, dd,  $J=11.2, 5.2$  Hz, H-5''<sub>eq</sub>), 3.60 (1H, m, H-6''), 3.53 (1H, dd,  $J=8.9, 7.3$  Hz, H-2''), 3.47 (1H, br t,  $J=8.9$  Hz, H-3''), and 3.40 (1H, dd,  $J=11.2, 10.4$  Hz, H-5''<sub>ax</sub>)]. The coupling constant between H-1'' and H-2'' ( $J=7.3$  Hz) is consistent with a  $\beta$ -configuration of the glycosidic bond, which is typical for xylose. The presence of a doublet of doublets at  $\delta_{\text{H}}$  3.97

(1H, dd,  $J=11.2, 5.2$  Hz, H-5''<sub>eq</sub>) and a doublet of doublets at  $\delta_{\text{H}}$  3.97 (1H, dd,  $J=11.2, 10.4$  Hz, H-5''<sub>ax</sub>) indicates a non-equivalent methylene group, characteristic of xylose. In contrast, arabinose would show a doublet for the equivalent methylene protons. The  $^{13}\text{C}$  NMR chemical shifts of the glycoside carbons ( $\delta_{\text{C}}$  103.0, 75.0, 78.4, 71.1, and 67.4) are in good agreement with the reported values for xylose [13].

The glycoside protons suggested that the pentose glycoside moiety was xylose. 20 carbon signals were obtained from  $^{13}\text{C}$  NMR spectrum and were assigned by a DEPT experiments as one oxygenated methylene, four oxygenated methine, eight olefinic methine, six tetra-substituted olefinic, one carbonyl. From the above structural characteristics, compound **4** was thus tentatively proposed to be a chalcone. The HMBC correlations between H-1'' ( $\delta_{\text{H}}$  5.08) /C-2', indicating the xylose attached to C-2'. Therefore, compound **4** was identified as chalconaringenin-2'-xyloside (Fig. 2) [14]. Compounds **1–4** in the flowers contained 0.22, 0.02, 0.26, and 0.10 mg/g, respectively.

To investigate the effects of ACF hot water extract on preadipocytes differentiation into mature adipocytes, post-confluent 3T3-L1 preadipocytes were exposed to various concentrations of extract throughout the differentiation

**Table 2**  $^1\text{H}$  and  $^{13}\text{C}$  NMR chemical shift data analysis result of chalconaringenin-2'-xyloside (**4**) ( $\delta$  in ppm,  $J$  in Hz, 400 and 100 MHz in  $\text{CD}_3\text{OD}$ )

| Position          | $\delta_{\text{C}}$ | $\delta_{\text{H}}$  | HMBC                             |
|-------------------|---------------------|----------------------|----------------------------------|
| 1                 | 128.7               |                      |                                  |
| 2                 | 131.8               | 7.59 d (8.6)         | C-1, C-3, C-4, C-6, C- $\beta$   |
| 3                 | 117.1               | 6.83 d (8.6)         | C-1, C-2, C-4, C-5,              |
| 4                 | 161.2               |                      |                                  |
| 5                 | 117.1               | 6.83 d (8.6)         | C-1, C-3, C-4, C-6,              |
| 6                 | 131.8               | 7.59 d (8.6)         | C-1, C-2, C-4, C-5, C- $\beta$   |
| 1'                | 107.7               |                      |                                  |
| 2'                | 161.9               |                      |                                  |
| 3'                | 96.3                | 6.16 d (2.4)         | C-1', C-2', C-4', C-5',          |
| 4'                | 166.8               |                      |                                  |
| 5'                | 98.8                | 5.99 d (2.4)         | C-1', C-3', C-4', C-6',          |
| 6'                | 168.0               |                      |                                  |
| $\alpha$          | 126.1               | 7.99 d (15.4)        | C-1, C=O, C- $\beta$             |
| $\beta$           | 144.2               | 7.67 d (15.4)        | C-1, C-2, C-6, C- $\alpha$ , C=O |
| C=O               | 194.4               |                      |                                  |
| 1''               | 103.0               | 5.08 d (7.3)         | C-2'                             |
| 2''               | 75.0                | 3.53 dd (8.9, 7.3)   | C-1'', C-3''                     |
| 3''               | 78.4                | 3.47 br t (8.9)      | C-2'', C-4''                     |
| 4''               | 71.1                | 3.60 m               | C-3''                            |
| 5'' <sub>eq</sub> | 67.4                | 3.97 dd (11.2, 5.2)  | C-1'', C-3'', C-4''              |
| 5'' <sub>ax</sub> |                     | 3.40 dd (11.2, 10.4) | C-1'', C-3''                     |

process (days 0–10). Upon completion of adipogenesis on day 10, the differentiated 3T3-L1 cells were stained with Oil Red O solution to quantify the accumulation of intracellular lipid droplets. The results showed the effects of treating cells with 45, 90, and 180  $\mu\text{g/ml}$  of extract, as well as the effect of the positive control quercetin (64  $\mu\text{M}$ ). As shown in Fig. 3, ACF hot water extract inhibited intracellular lipid droplet accumulation in a dose-dependent manner. Moreover, compared with fully differentiated adipocytes, the extract at 45, 90, and 180  $\mu\text{g/ml}$  of extract decreased the lipid content in 3T3-L1 cells by 18.7%, 22.2%, and 30.7%, respectively. To confirm whether the effect of ACF hot water extract in inhibiting adipogenesis was due to cytotoxicity, the cell viability of 3T3-L1 cells was measured by thiazolyl blue tetrazolium bromide (MTT) assay after treatment with the extract. The findings revealed that the extract did not exhibit significant cytotoxicity up to a concentration of 180  $\mu\text{g/ml}$ , with cell viability remaining above 90% for all tested concentrations (Fig. 3c). Although a slight dose-dependent decrease in cell viability was observed, it is unlikely to have a substantial impact on the results presented in Fig. 3b, as the viability remained high throughout the tested range.

During the early stage of 3T3-L1 cells adipocyte differentiation, transcription factors from the *CCAT/ehancer binding protein (C/EBP)* family were initially expressed.

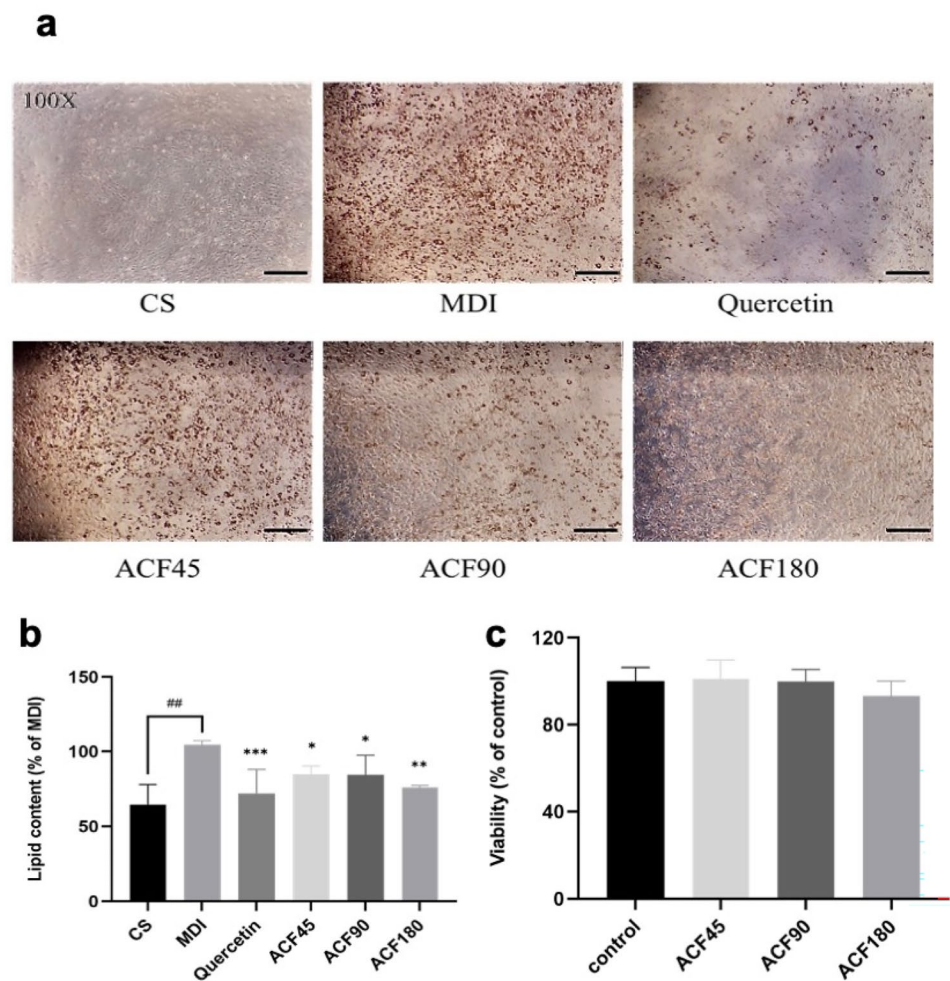
As shown in Fig. 4, upon induction by the differentiation cocktail (3-isobutyl-1-methylxanthine, dexamethasone, insulin, MDI), *C/EBP $\beta$* , *C/EBP $\delta$*  and *C/EBP $\alpha$*  genes were highly upregulated, while treatment with ACF hot water extract suppressed their expression. Compared to the MDI group, extract and quercetin slightly decreased *C/EBP $\beta$*  gene expression (Fig. 4b). For *C/EBP $\delta$* , extract treatment reduced expression compared to MDI in a dose-dependent manner, with 180  $\mu\text{g/ml}$  extract suppressing it by approximately 50%, similar to quercetin (Fig. 4c). The extract also downregulated *C/EBP $\alpha$* , although not as potently as the positive control quercetin (Fig. 4a).

In the late differentiation stage, lipogenic transcription factors like *sterol regulatory element binding protein-1c (SREBP-1c)*, lipogenic genes such as *acetyl-CoA carboxylase 1 (ACCI)*, *fatty acid synthase (FAS)*, *stearoyl-CoA desaturase 1 (SCD1)*, as well as adipocyte markers *fatty acid translocase (CD36)* and *adiponectin* were expressed. As shown in Fig. 4d–g, the extract suppressed lipogenic gene expressions. Treatment with extract inhibited *SREBP-1c* expression in a dose-dependent manner (Fig. 4d). Concurrently, the extract downregulated *ACCI*, *FAS* and *SCD1*, with higher concentrations exhibiting greater inhibition (Fig. 4e, f, and g). Although the extract did not significantly reduce *CD36* and *adiponectin* compared to the positive control, their expression was lower than the MDI group (Fig. 4h and i). Since lipid synthesis requires lipogenic enzymes, the downstream protein expression of ACC, FAS, and CD36 were analyzed. The results (Fig. 5a, b, and c) showed that ACF hot water extract significantly inhibited ACC, FAS, and CD36 protein levels at higher concentrations (180  $\mu\text{g/ml}$ ). The expression of the transcription factors peroxisome proliferation-activated receptor  $\gamma$  (PPAR $\gamma$ ) and SREBP-1, which are upregulated during mid-differentiation, were also examined. The key adipogenic transcription factor PPAR $\gamma$ , acting as a dimer, was downregulated by ACF90 and ACF180 treatments for both PPAR $\gamma$ 1 and PPAR $\gamma$ 2 isoforms (Fig. 5d). Additionally, *C/EBP $\alpha$*  was inhibited in a dose-dependent manner, with higher extract concentrations showing greater suppression (Fig. 5e). We also assessed the effects of the ACF hot water extract on the protein levels of SREBP-1, *C/EBP $\beta$* , *C/EBP $\delta$* , pAMPK, pCREB, and GR. However, due to the lack of a significant response in the positive control group, the effects of the extract on these proteins remain inconclusive and require further validation with more effective positive controls. In summary, the ACF hot water extract inhibited the expression of key proteins involved in the early and mid-stages of adipogenesis, including PPAR $\gamma$ , *C/EBP $\alpha$* , ACC, FAS, and CD36. These findings suggest that ACF hot water extract may be a natural source of active compounds for developing novel anti-obesity drugs.

Based on the literature evidence suggesting that the major compounds in *A. confusa* flowers are flavonoids and



**Fig. 3** The effect of *A. confusa* flowers hot water extract on 3T3-L1 preadipocytes during differentiation. After treating for 8 days in MDI induction medium, the lipid accumulation was measured by Oil Red O staining (a) and relative lipid content were quantified (b). The cell viability of 3T3-L1 preadipocytes treated with *A. confusa* flowers hot water extract at concentration of 45 (ACF45), 90 (ACF90) and 180 (ACF180)  $\mu\text{g/ml}$  was evaluated (c). Values were expressed as the means  $\pm$  SD. \* $P < 0.05$  versus MDI (differentiation control). \*\* $P < 0.01$  versus MDI. \*\*\* $P < 0.001$  versus MDI. ## $P < 0.01$  versus CS (untreated control)



flavonoid glycosides [9]. Flavonoids and their glycosides have been reported to possess various biological activities, including anti-obesity effects [15]. Given this background information, we selected 360 nm as the detection wavelength for our HPLC analysis, as it is suitable for the detection of flavonoids and their glycosides. The HPLC chromatogram at 360 nm revealed that compound 1–4 were major peaks, suggesting its relative abundance in the ACF hot water extract. Literature reports suggest that myricitrin and europetin-3-*O*-rhamnoside may not have the ability to inhibit lipid formation and could even promote adipocyte differentiation [16]. Quercitrin has been reported to inhibit lipid formation, but its content in ACF is extremely low. Since quercitrin is a glycosylated derivative of quercetin, which had the ability to inhibit lipid formation, we also detected the presence of quercetin in the extract, but the result was not found. Therefore, we hypothesize that the compound primarily responsible for inhibiting lipid formation is chalconaringenin-2'-xyloside. This study provides valuable insights into the major compounds present in the *A. confusa* flower hot water extract and their potential contributions to

the observed anti-lipogenic effects. However, it is important to note that the HPLC results at other UV wavelengths were not shown in our study, and therefore, it cannot be definitively concluded that compound 4 is the most abundant compound overall or the primary contributor to the anti-lipogenic activity. To conclusively identify the specific active compounds responsible for the inhibition of lipid accumulation in 3T3-L1 cells, further studies employing bioassay-guided fractionation and isolation are necessary. These future investigations will not only help confirm the specific role of compound 4 and other constituents in the inhibition of lipid formation but also provide a more comprehensive understanding of the active components within the extract. Despite these limitations, our findings lay a strong foundation for the development of ACF hot water extract as a potential source of anti-obesity agents and pave the way for further research in this area.

We reviewed several studies on the inhibition of lipid accumulation in 3T3-L1 cells by flowers extract from different plants. According to the research, the *Chrysanthemum morifolium* flowers hot water extract inhibited lipid

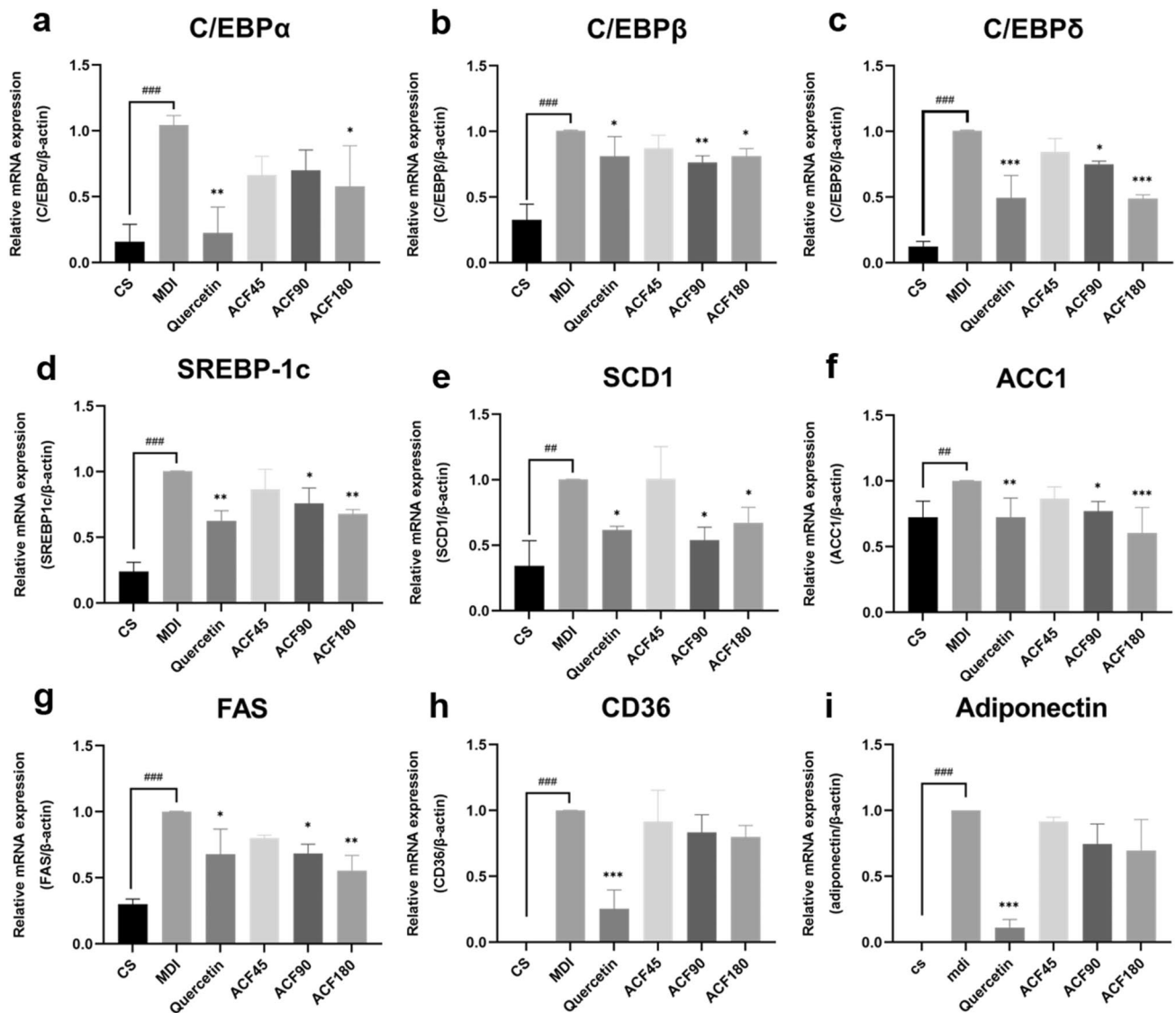


**Fig. 4** The effect of *A. confusa* flowers hot water extract on mRNA expression levels during 3T3-L1 preadipocyte differentiation, determined by real-time PCR. After 2 days treatment, mRNA levels of (a) *C/EBP $\alpha$* , (b) *C/EBP $\beta$*  and (c) *C/EBP $\delta$*  were measured. After 6 days of treatment, mRNA levels of (d) *SREBP-1c*, (e) *SCD1*, (f)

*ACC1*, (g) *FAS*, (h) *CD36*, (i) *Adiponectin* were measured. Values were expressed as means  $\pm$  SD. \* $P < 0.05$  versus MDI (differentiation control). \*\* $P < 0.01$  versus MDI. \*\*\* $P < 0.001$  versus MDI. ### $P < 0.001$  versus CS (untreated control). ACF45, 45  $\mu$ g/ml. ACF90, 90  $\mu$ g/ml. ACF180, 180  $\mu$ g/ml

accumulation in 3T3-L1 cells at a concentration as low as 1  $\mu$ g/ml, acting through the activation of the AMPK/NAD-dependent deacetylase sirtuin-1 (SIRT1) pathway [17]. The *Clitoria ternatea* flowers hot water extract inhibited 26.40% of lipid formation at 500  $\mu$ g/ml and 68.25% at 1000  $\mu$ g/ml, by downregulating the expression of phospho-RAC-alpha serine/threonine-protein kinase (pAkt1) and phospho-extracellular signal-regulated protein kinases 1 and 2 (pERK1/2) proteins [18]. The *Prunus persica* flowers hot water extract inhibited 22.66% of lipid formation at 25  $\mu$ g/ml and 86.09% at 100  $\mu$ g/ml, by reducing the expression of p-ERK, phospho-Jun N-terminal kinase (p-JNK),

phospho-p38 mitogen-activated protein kinases (p-P38), and GR proteins [19]. In our study, the ACF hot water extract inhibited 18.7%, 22.2%, and 30.7% of lipid formation at 45, 90, and 180  $\mu$ g/ml, respectively, performing better than *Clitoria ternatea* flowers extract but worse than *Chrysanthemum morifolium* flowers and *Prunus persica* flowers extract. It is worth noting that our extraction time was only 15 min, while most other studies extracted for over an hour [17–19]. The shorter extraction time in our study may have influenced the extraction efficiency of potential active compounds, and consequently, the effective concentration of the extract. However, as the specific active compounds

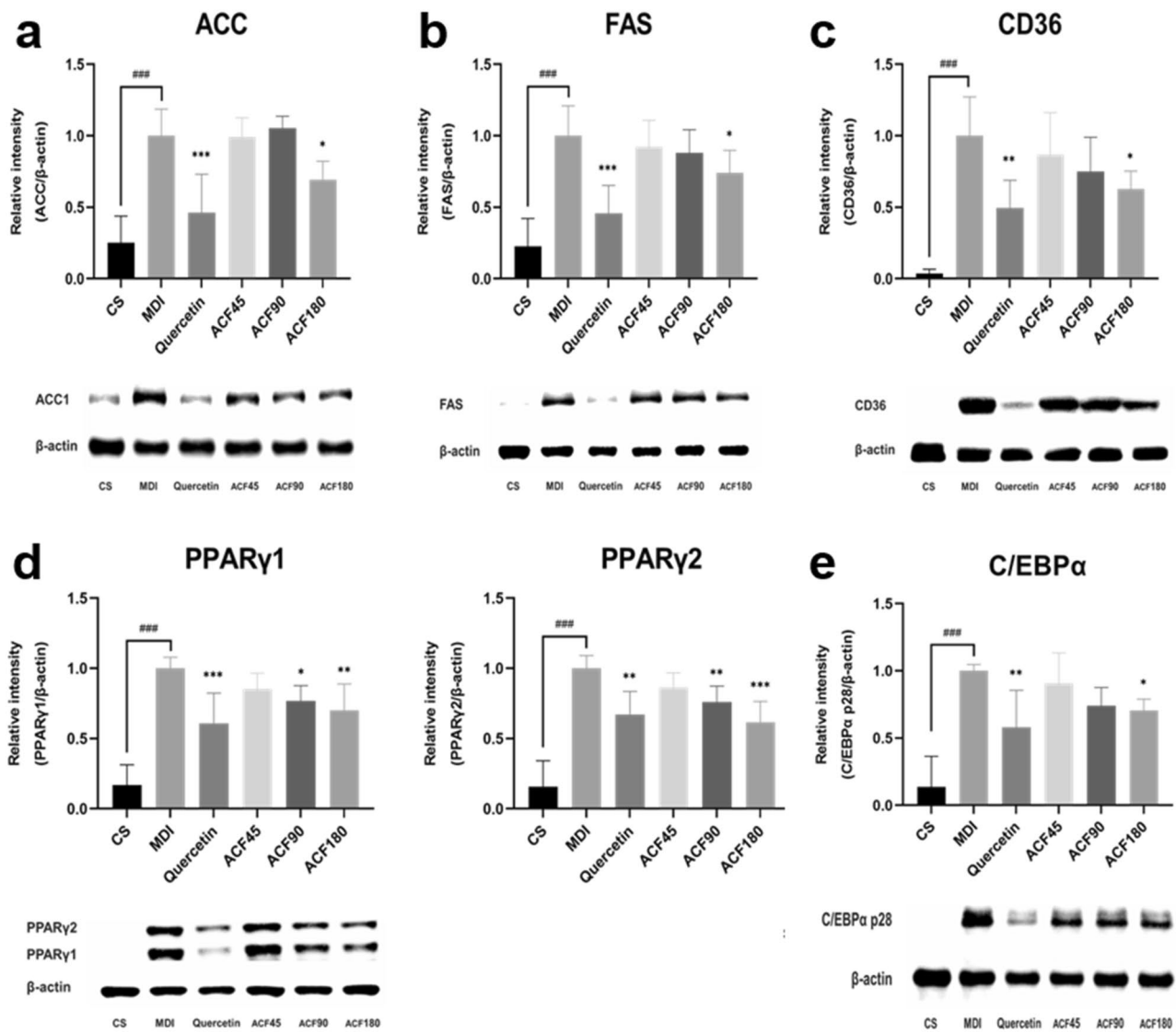


**Fig. 5** The effect of *A. confusa* flowers hot water extract on protein levels of (a) ACC, (b) FAS, (c) CD36, (d) PPAR $\gamma$ , (e) C/EBP $\alpha$  during 3T3-L1 preadipocyte differentiation. Proteins were isolated on day 8 after inducing differentiation (MDI) and analyzed by western blotting. CS represents untreated control cells. Values are expressed

as means  $\pm$  SD.  $P < 0.05$  versus MDI (differentiation control).  $*P < 0.01$  versus MDI.  $**P < 0.001$  versus MDI.  $###P < 0.001$  versus CS (untreated control). ACF45, 45  $\mu$ g/ml. ACF90, 90  $\mu$ g/ml. ACF180, 180  $\mu$ g/ml

responsible for the anti-lipogenic effects of ACF hot water extract have not been conclusively identified, further studies are needed to elucidate the relationship between extraction parameters, active compounds, and biological activity.

This study primarily focused on investigating the anti-obesity potential of ACF hot water extract and elucidating its mechanism of action. Our results demonstrated that the extract significantly inhibited lipid accumulation in 3T3-L1 cells, suppressed adipogenic transcription factors, and downregulated lipogenic enzymes, underscoring its promising anti-obesity effects. While we identified several major compounds in the extract, the emphasis was placed

on the overall bioactivity of the extract rather than the specific contributions of individual components. Further studies involving bioassay-guided fractionation and isolation are needed to conclusively identify the active compounds responsible for the observed anti-obesity effects. Nevertheless, this study offers valuable insights into the anti-obesity potential of ACF hot water extract and its underlying mechanisms, laying the groundwork for the development of this natural extract as a potential therapeutic agent for the prevention and treatment of obesity and related metabolic disorders.



## Materials and methods

### Collection and extraction of ACF

ACF were gathered from the wild in Dadu District, Taichung City, during the flowering period in April and May 2021. The flowers and branches were manually separated, and only mature, yellow, ball-shaped flowers were selected for collection. Upon harvesting, hot water extraction was immediately conducted. The collected ACF, weighing 100 g, were placed in an Erlenmeyer flask. Subsequently, 1000 ml of hot water was added, and extraction took place in an 80 °C water bath for 15 min. The resulting extract was filtered using vacuum-assisted filter paper to eliminate impurities. Finally, the filtrate was subjected to freeze-drying to remove water content and obtain the final extract. The yield of ACF hot water extract was approximately 6.02% (w/w) based on the flowers.

### Analysis and identification of components in ACF hot water extract

#### Separation and purification of ACF hot water extract

The hot water extract obtained from ACF were subjected to separation and purification using Agilent HPLC. Compounds were separated using a C<sub>18</sub> column (Cosmosil 5C<sub>18</sub>-AR-II, Nacalai Tesque, INC), and different compounds were collected at various time points. The two solvents systems were conducted to separate hot water extract, methanol (A) and H<sub>2</sub>O (B). The gradient elution profile was as follows: 0–5 min, 45% A in B (isocratic); 5–15 min, 45–50% A to B (linear gradient); 15–20 min, 50% A in B (isocratic); 20–50 min 70–30% A to B (linear gradient); 30–50 min, 70–100% A in B (linear gradient); the flow rate was 1.5 ml/min and the detector wavelength was set at 360 nm. The major compounds in the hot water extract were obtained at retention times of 7.0 min (**1**), 9.0 min (**2**), 9.5 min (**3**), and 9.9 min (**4**). The weights of isolated compounds **1**, **2**, **3**, and **4** were 13 mg, 6 mg, 10 mg, and 8 mg, respectively.

#### Identification and quantification of the main components in ACF hot water extracts

The structures of compounds **1** to **4** (Fig. 1) were then elucidated using spectroscopic analyses. HR-MS was determined using an LTQ Orbitrap XL (Thermo Fisher Scientific, Waltham, Massachusetts, U.S.) and NMR spectra recorded with a Bruker AVANCE III NMR spectrometer (Bruker, Billerica, Massachusetts, US), acquiring <sup>1</sup>H data at 400 MHz and <sup>13</sup>C data at 100 MHz, using standard experiments from

Bruker pulse programs library. For calibration curves, appropriate volumes of the standard stock solutions (2 mg/ml) were diluted with deionized water, and five concentration levels (100, 250, 500, 1000 and 2000 µg/ml) were analyzed. For quantification, the peak areas were correlated with the concentrations according to the calibration curve. All data are expressed as mean ± standard deviation of triplicate independent experiments (*n* = 3).

### Cell culture and stimulation

The 3T3-L1 cells were obtained from the Bioresource Collection and Research Center in Hsinchu, Taiwan. These cells were cultured in Dulbecco's Modified Eagle's Medium (DMEM), supplemented with 10% bovine serum (BS), 100 units/ml penicillin, and 100 µg/ml streptomycin (GIBCO, Invitrogen, Carlsbad, CA), and maintained at 37 °C in a 5% CO<sub>2</sub>-humidified incubator. Cell differentiation was induced using a combination of 1 µmol/L dexamethasone, 0.52 mmol/L isobutylmethylxanthine, and 0.17 µmol/L insulin (Sigma-Aldrich), starting from 2 days post-confluence and continuing for 4 days (from day 3 to day 6). Following this stimulation period, the medium was replaced with maintenance medium (DMEM supplemented with 10% FBS) for an additional 4 days (from day 7 to day 10). To evaluate the effect of the hot water extracts on adipogenesis, the specified concentrations of extracts were added on both day 3 and day 7 during the medium refreshment.

### Oil Red O staining

The 3T3-L1 adipocytes were rinsed with phosphate buffered saline (PBS) and subsequently fixed with 4% paraformaldehyde for 1 h at room temperature. After discarding the supernatant, the cells were washed with deionized water. Subsequently, the cells were stained for 10 min at room temperature using a freshly prepared 0.3% Oil Red O solution. To quantify the relative lipid content accumulated in the cells, the Oil Red O dye was eluted with 100% isopropanol. The eluate was then incubated for 10 min with gentle shaking, and the absorbance at 510 nm was measured using an ELISA microplate reader (µQuant, Bio-Tek Instruments, Winooski, VT). The results were validated through three independent experiments.

### Cell toxicity assay

To assess the cytotoxicity of the hot water extracts obtained from ACF on 3T3-L1 cells, the following method was employed. 3T3-L1 cells were seeded into 48-well plates at a density of 5000 cells per well and incubated at 37 °C with 5% CO<sub>2</sub>. After confluence, the cells were treated with varying concentrations of the ACF hot water extracts (45,

90, and 180  $\mu\text{g/ml}$ ) for 48 h. After the treatment period, each well was change to with 0.5 mg/ml of MTT solution in medium, followed by a 2 h incubation. Subsequently, the excess MTT solution was aspirated, and the formazan crystals formed were dissolved using 200  $\mu\text{L}$  of dimethyl sulfoxide (DMSO) with gentle shaking for 5 min. The absorbance at 570 nm was then measured using an ELISA microplate reader ( $\mu\text{Quant}$ , Biotek Instruments, Winooski, VT, USA) to assess cell viability. The percentage of cell viability (%) was calculated as  $A_{570}$  of treated cells /  $A_{570}$  of untreated cells  $\times$  100.

### Quantitative Real-Time PCR

Cellular total mRNA was extracted from 3T3-L1 cells after confluence at day 2 and day 6, using a total RNA purification kit (GeneMark, New Taipei City, Taiwan). RNA was quantified with a NanoVue Plus spectrophotometer (GE Health Care Life Sciences, Chicago, IL, USA). Complementary DNA (cDNA) was synthesized with the SuperScript IV reverse transcriptase kit (Invitrogen) following the manufacturer's instructions. Gene expression levels were analyzed using the StepOne Real-Time PCR System (Applied Biosystems, Foster City, CA, USA). The analyses for the genes  *$\beta$ -actin*, *C/EBP $\alpha$* , *C/EBP $\beta$* , *C/EBP $\delta$* , *ACCI*, *FAS*, *SREBP1-c*, *CD36*, *SCD1*, *Adiponectin* were conducted using PowerUp SYBR Green Master Mix (Applied Biosystems, Foster City, CA, USA) [20–26]. The cDNA was denatured at 94  $^{\circ}\text{C}$  for 4 min, followed by 40 cycles of amplification of 94  $^{\circ}\text{C}$  for 30 s and 60  $^{\circ}\text{C}$  for 30 s. Sample normalization was performed using the  *$\beta$ -actin* endogenous control. The relative abundance of target mRNA for each sample was determined using the  $2^{-\Delta\Delta\text{Ct}}$  method.

### Protein extraction and immunoblotting

3T3-L1 cells were cultured in 6 cm dishes at a density of  $8 \times 10^4$  cells. After confluence, differentiation was induced using MDI, and cells were treated with the ACF hot water extracts on day 3 and 7. Total proteins were extract from day 1–8 using lysis buffer (Thermo Fisher Scientific, Waltham, MA, USA) supplemented with 1% protease inhibitor cocktail and 1% phosphatase protease inhibitor. Protein concentrations were determined using the Bradford protein assay (Bio-Rad, Hercules, CA, USA) according to the manufacturer's instructions. A total of 80  $\mu\text{g}$  of protein was separated by 8% or 10% sodium dodecyl sulfate–polyacrylamide gel electrophoresis (SDS-PAGE) and transferred onto polyvinylidene difluoride (PVDF; Merck Millipore, Burlington, MA, USA) membranes at 300 mA for 120 min. The membranes were blocked with blocking buffer (5% w/v skim milk in TBST) for 90 min at room temperature, follow by overnight incubation with primary antibody at 4  $^{\circ}\text{C}$ . Primary antibodies

included anti- $\beta$ -actin (A5441) and anti-AMPK $\alpha$ 1 (#07–350) from Millipore Sigma, anti-ACC (#3662), anti-FAS (#3180), anti-C/EBP $\alpha$  (#8178), anti-C/EBP $\beta$  (#3087), anti-C/EBP $\delta$  (#2318), anti-PPAR $\gamma$  (#2443), anti-p-AMPK $\alpha$  (#2535), anti-CREB (#9197), and anti-p-CREB (#9198) from Cell Signaling, anti-CD36 (GTX112891) from GeneTex, anti-SREBP-1 (sc-366) and anti-GR (sc-393232) from Santa cruz. After washing with TBST three times, the membranes were incubated with secondary antibodies (anti-rabbit or anti-mouse conjugated with horseradish peroxidase) for 2 h. Protein bands were detected by immobilon western chemiluminescent HRP substrate (Merck Millipore), visualized using ChemiDoc XRS + docking system (Bio-Rad), and quantified by Imagelab software (Bio-Rad).

### Statistical analysis

The data are presented as mean  $\pm$  standard deviation (mean  $\pm$  SD) of three independent experiments. Statistical analysis and graphing were performed using GraphPad Prism 9 (GraphPad Software, San Diego, CA). Student's t-test was employed to compare the control group (CS) with the MDI-induced group (MDI). One-way analysis of variance (One-way ANOVA) was conducted to compare the MDI-induced group with each treatment group. Dunnett's multiple test method was used for post-hoc analysis to assess differences among the treatment groups. Statistical significance was defined as  $p < 0.05$ .

**Acknowledgements** We thank Dr. Wen-Wei Hsiao for collecting *A. confusa* flowers.

**Author contributions** N-WT and J-YC contributed to perform the experiments and analyze the data. N-WT and S-YW designed the experiments and supervised the study. N-WT, J-YC and S-YW wrote the manuscript. All the authors contributed to the article and agreed to submit this version.

**Funding** This work was supported by the grant from the Taichung Branch, Forestry and Nature Conservation Agency, Ministry of Agriculture, (1101B028), Taiwan.

### Declarations

**Conflict of interest** All authors declare no competing of interests.

### References

1. Lin HY, Chang TC, Chang ST (2018) A review of antioxidant and pharmacological properties of phenolic compounds in *Acacia confusa*. J Tradit Compl Med 8:443–450. <https://doi.org/10.1016/j.jtcme.2018.05.002>
2. Lin HY, Chang ST (2013) Antioxidant potency of phenolic phytochemicals from the root extract of *Acacia confusa*. Ind Crop Prod 49:871–878. <https://doi.org/10.1016/j.indcrop.2013.07.001>
3. Chang ST, Wu JH, Wang SY, Kang PL, Yang NS, Shyur LF (2001) Antioxidant activity of extracts from *Acacia confusa* bark

- and heartwood. *J Agr Food Chem* 49:3420–3424. <https://doi.org/10.1021/jf0100907>
4. Wu JH, Huang CY, Tung YT, Chang ST (2008) Online RP-HPLC-DPPH screening method for detection of radical-scavenging phytochemicals from flowers of *Acacia confusa*. *J Agr Food Chem* 56:328–332. <https://doi.org/10.1021/jf072314c>
  5. Tung YT, Wu JH, Huang CC, Peng HC, Chen YL, Yang SC, Chang ST (2009) Protective effect of *Acacia confusa* bark extract and its active compound gallic acid against carbon tetrachloride-induced chronic liver injury in rats. *Food Chem Toxicol* 47:1385–1392. <https://doi.org/10.1016/j.fct.2009.03.021>
  6. Tung YT, Chang ST (2010) Inhibition of xanthine oxidase by *Acacia confusa* extracts and their phytochemicals. *J Agr Food Chem* 58:781–786. <https://doi.org/10.1021/jf901498q>
  7. Tung YT, Hsu CA, Chen CS, Yang SC, Huang CC, Chang ST (2010) Phytochemicals from *Acacia confusa* heartwood extracts reduce serum uric acid levels in oxonate-induced mice: their potential use as xanthine oxidase inhibitors. *J Agr Food Chem* 58:9936–9941. <https://doi.org/10.1021/jf102689k>
  8. Wu JH, Tung YT, Chien SC, Wang SY, Kuo YH, Shyur LF, Chang ST (2008) Effect of phytocompounds from the heartwood of *Acacia confusa* on inflammatory mediator production. *J Agr Food Chem* 56:1567–1573. <https://doi.org/10.1021/jf072922s>
  9. Tung YT, Chang WC, Chen PS, Chang TC, Chang ST (2011) Ultrasound-assisted extraction of phenolic antioxidants from *Acacia confusa* flowers and buds. *J Sep Sci* 34:844–851. <https://doi.org/10.1002/jssc.201000820>
  10. El-Kashak W, Hamed AR, El-Raey M, Elshamy AI, Abd-Ellatef GEF (2016) Antiproliferative, antioxidant and antimicrobial activities of phenolic compounds from *Acrocarpus fraxinifolius*. *J Chem Pharm Res* 8:520–528. <https://doi.org/10.1186/s13568-019-0924-0>
  11. Shen CJ, Chen CK, Lee SS (2009) Polar constituents from *Sageretia thea* leaf characterized by HPLC-SPE-NMR assisted approaches. *J Chin Chem Soc-Taip* 56:1002–1009. <https://doi.org/10.1002/jccs.200900146>
  12. Agrawal PK (1992) NMR spectroscopy in the structural elucidation of oligosaccharides and glycosides. *Phytochemistry* 31:3307–3330. [https://doi.org/10.1016/0031-9422\(92\)83678-R](https://doi.org/10.1016/0031-9422(92)83678-R)
  13. Da Costa EV, Moreira ASP, Nunes FM, Coimbra MA, Evtuguin DV, Domingues MRM (2007) Differentiation of isomeric pentose disaccharides by electrospray ionization tandem mass spectrometry and discriminant analysis. *J Am Soc Mass Spectrom* 18:1279–1292. <https://doi.org/10.1002/rcm.6415>
  14. Rosa W, da Silva DO, de Oliveira SPP, Caldas IS, Murgu M, Lago JHG, Sartorelli P, Dias DF, Chagas-Paula DA, Soares MG (2021) *In vivo* anti-inflammatory activity of Fabaceae species extracts screened by a new *ex vivo* assay using human whole blood. *Phytochem Anal* 32:859–883. <https://doi.org/10.1002/pca.3031>
  15. Kawser Hossain M, Abdal Dayem A, Han J, Yin Y, Kim K, Kumar Saha S, Yang GM, Choi HY, Cho SG (2016) Molecular mechanisms of the anti-obesity and anti-diabetic properties of flavonoids. *Int J Mol Sci* 17:569. <https://doi.org/10.3390/ijms17040569>
  16. Manaharan T, Ming CH, Palanisamy UD (2013) *Syzygium aqueum* leaf extract and its bioactive compounds enhances pre-adipocyte differentiation and 2-NBDG uptake in 3T3-L1 cells. *Food Chem* 136:354–363. <https://doi.org/10.1016/j.foodchem.2012.08.056>
  17. Lee MS, Kim Y (2020) *Chrysanthemum morifolium* flower extract inhibits adipogenesis of 3T3-L1 cells via AMPK/SIRT1 pathway activation. *Nutrients* 12:2726. <https://www.mdpi.com/2072-6643/12/9/2726>.
  18. Chayaratanasin P, Caobi A, Suparpprom C, Saenset S, Pasukamonset P, Suanpairintr N, Barbieri MA, Adisakwattana S (2019) *Clitoria ternatea* flower petal extract inhibits adipogenesis and lipid accumulation in 3T3-L1 preadipocytes by downregulating adipogenic gene expression. *Molecules* 24:1894. <https://www.mdpi.com/1420-3049/24/10/1894>.
  19. Lee D, Kim JY, Qi Y, Park S, Lee HL, Yamabe N, Kim H, Jang DS, Kang KS (2021) Phytochemicals from the flowers of *Prunus persica* (L.) Batsch: Anti-adipogenic effect of mandelamide on 3T3-L1 preadipocytes. *Bioorg Med Chem Lett* 49:128326. <https://doi.org/10.1016/j.bmcl.2021.128326>
  20. Cho Y, Ariga M, Uchijima Y, Kimura K, Rho JY, Furuhashi Y, Hakuno F, Yamanouchi K, Nishihara M, Takahashi SI (2006) The novel roles of liver for compensation of insulin resistance in human growth hormone transgenic rats. *Endocrinology* 147(5374–5384):5374–5384. <https://doi.org/10.1210/en.2006-0518>
  21. Lee J, Jung E, Lee J, Kim S, Huh S, Kim Y, Kim Y, Byun SY, Kim YS, Park D (2009) Isorhamnetin represses adipogenesis in 3T3-L1 cells. *Obesity* 17:226–232. <https://doi.org/10.1038/oby.2008.472>
  22. Inokawa A, Inuzuka T, Takahara T, Shibata H, Maki M (2016) Tubby-like protein superfamily member PLSCR3 functions as a negative regulator of adipogenesis in mouse 3T3-L1 preadipocytes by suppressing induction of late differentiation stage transcription factors. *Bioscience Rep* 36:e00287. <https://doi.org/10.1042/bsr20150215>
  23. Qiao LP, MacLean PS, You HN, Schaack J, Shao JH (2006) Knocking down liver CCAAT/enhancer-binding protein  $\alpha$  by adenovirus-transduced silent interfering ribonucleic acid improves hepatic gluconeogenesis and lipid homeostasis in *db/db* mice. *Endocrinology* 147:3060–3069. <https://doi.org/10.1210/en.2005-1507>
  24. Li KK, Liu CL, Shiu HT, Wong HL, Siu WS, Zhang C, Han XQ, Ye CX, Leung PC, Ko CH (2016) Cocoa tea (*Camellia pitlophylla*) water extract inhibits adipocyte differentiation in mouse 3T3-L1 preadipocytes. *Sci Rep* 6:20172. <https://doi.org/10.1038/srep20172>
  25. Pachikian BD, Neyrinck AM, Cani PD, Portois L, Deldicque L, De Backer FC, Bindels LB, Sohet FM, Malaisse WJ, Francaux M, Carpentier YA, Delzenne NM (2008) Hepatic steatosis in n-3 fatty acid depleted mice: focus on metabolic alterations related to tissue fatty acid composition. *BMC Physiol* 8:21. <https://doi.org/10.1186/1472-6793-8-21>
  26. Qiao LP, Zou CH, van der Westhuyzen DR, Shao JH (2008) Adiponectin reduces plasma triglyceride by increasing VLDL triglyceride catabolism. *Diabetes* 57:1824–1833. <https://doi.org/10.2337/db07-0435>

**Publisher's Note** Springer Nature remains neutral with regard to jurisdictional claims in published maps and institutional affiliations.